Magnetic Resonance Imaging 62 (2019) 199–208

Contents lists available at ScienceDirect

Magnetic Resonance Imaging

journal homepage: www.elsevier.com/locate/mri

Original contribution

Diffusional kurtosis imaging for differentiation of additional suspicious lesions on preoperative breast MRI of patients with known breast cancer

Vivian Youngjean Park[a], Sungheon G. Kim[b], Eun-Kyung Kim[a], Hee Jung Moon[a], Jung Hyun Yoon[a], Min Jung Kim[a,*]

[a] Department of Radiology and Research Institute of Radiological Science, Severance Hospital, Yonsei University College of Medicine, South Korea
[b] Center for Advanced Imaging Innovation and Research (CAI2R), New York University School of Medicine, New York, NY 10016, United States

ARTICLE INFO

Keywords:
Diffusional kurtosis imaging
Breast
MRI
Preoperative
Diffusion-weighted imaging

ABSTRACT

Purpose: To investigate the potential of diffusional kurtosis imaging (DKI) and conventional diffusion-weighted imaging (DWI) in the evaluation of additional suspicious lesions at preoperative breast magnetic resonance imaging (MRI) in patients with breast cancer.

Materials and methods: Fifty-three additional suspicious lesions in 45 patients with breast cancer, which were detected on preoperative breast MRI, were examined with a 3-T MR system. DKI and DWI data were obtained using a spin-echo single-shot echo-planar imaging sequence with b-values of 0, 50, 600, 1000, and 3000 s/mm^2. Histogram parameters (mean, standard deviation, minimum, maximum, 10th, 25th, 50th, 75th, 90th percentiles, kurtosis, skewness and entropy) of ADC from DWI and diffusivity (D), kurtosis (K) from DKI were calculated after postprocessing. Parameters were compared between benign vs. ductal carcinoma in situ (DCIS) vs. invasive breast lesions and diagnostic performances were evaluated by receiver operating characteristic (ROC) analysis. Correlation between the mean values of D and K was analyzed according to lesion type.

Results: Multiple histogram parameters of D (mean, 25th, 50th percentile, 75th percentile, and entropy) differed between benign and invasive breast lesions (all $P < 0.005$), but none differed between benign vs. DCIS. D-90th percentile differed between DCIS vs. invasive cancer ($P = 0.040$). K-10th percentile differed between benign vs. DCIS ($P = 0.015$). ADC-75th percentile differed between benign vs. invasive cancer and ADC-75th percentile, ADC-90th percentile differed between DCIS vs. invasive cancer, respectively (all $P < 0.005$). ROC curve analysis showed high specificity for discrimination between benign and invasive cancer. D-mean and K-mean showed strong correlation in benign ($r_s = -0.813$) and invasive lesions ($r_s = -0.853$), but no significant correlation in DCIS.

Conclusion: DKI may aid in the differentiation of additional suspicious lesions at preoperative breast MRI. Both ADC and DKI may have lower potential in differentiating DCIS from benign lesions.

1. Introduction

Breast magnetic resonance (MR) imaging is the most sensitive imaging tool for detecting breast cancer, with a sensitivity of close to 100% [1,2]. In patients with newly diagnosed breast cancer, dynamic contrast material-enhanced (DCE) MR imaging has been reported to detect additional disease in the ipsilateral breast in 6%–34% and in the contralateral breast in 3%–6% of patients [3–6]. Although the clinical importance of additional diseases detected at MR imaging is still under debate [7–11], the majority of multicentric cancers detected only on MR imaging are invasive cancers and approximately 25% have been reported to be larger than in 1 cm [12]. In a meta-analysis of 3253 women, 64.9% of MR imaging-detected contralateral cancers were also reported to be invasive cancers [5]. Yet, DCE-MR imaging has lower and variable specificity for diagnosing breast cancer, and false-positive findings may lead to additional investigations or surgery [5,6,13].

Diffusion-weighted imaging (DWI) has been proposed to improve the specificity of breast MRI exams [14,15]. Conventional DWI can be used to measure apparent diffusion coefficient (ADC) values, which have been shown to differ significantly between benign and malignant breast lesions [16]. Although conventional DWI assumes a Gaussian diffusion of water protons, water diffusion in complex biological tissues

* Corresponding author at: Department of Radiology, Research Institute of Radiological Science, Yonsei University, College of Medicine, 50-1 Yonsei-ro, Seodaemun-gu, 03722 Seoul, South Korea.
E-mail address: mines@yuhs.ac (M.J. Kim).

https://doi.org/10.1016/j.mri.2019.07.011
Received 20 August 2018; Received in revised form 2 July 2019; Accepted 14 July 2019

shows a non-Gaussian phenomena, likely associated with tissue microstructure [17,18]. Diffusion kurtosis imaging (DKI) is a non-Gaussian diffusion weighted analysis method and includes calculation of diffusivity (*D*, diffusion coefficient with correction of non-Gaussian bias) and kurtosis (*K*, deviation of tissue diffusion from a Gaussian pattern) [19]. Several recent studies have reported that DKI improved the characterization of breast lesions [18–20], with one study reporting a higher specificity of DKI than that of conventional DWI [19]. However, no previous studies have investigated whether DKI could also be used to differentiate additional suspicious lesions detected at preoperative breast DCE-MR imaging in breast cancer patients. Therefore, the purpose of this study was to investigate the potential of DKI and conventional DWI in the evaluation of additional suspicious lesions detected at preoperative breast MR imaging in patients with newly diagnosed breast cancer.

2. Materials and methods

2.1. Study population

This retrospective study was approved by the institutional review board, and the requirement for informed consent was waived. Between July 2014 and September 2016, 1096 consecutive women with newly diagnosed breast cancer underwent preoperative breast MR imaging using a 3-T MR scanner (Ingenia, Philips Medical Systems, Best, The Netherlands). Among them, 194 patients underwent biopsy or surgery for additional suspicious breast lesions detected by breast MR imaging. Considering challenges in depiction of small lesions due to limited spatial resolution and lower SNR with the use of higher b values [21–23], we excluded 149 patients with lesions smaller than 10 mm. Finally, 45 patients (mean age, 46 years; range, 29–65 years) with 53 pathologically confirmed (confirmed by surgery [n = 28], US-guided vacuum-assisted biopsy [n = 2] and core needle biopsy [n = 23]) additional suspicious breast lesions ≥10 mm, which were detected by preoperative breast MRI imaging, were included in our study.

2.2. MRI acquisition protocol

Imaging was performed by using a 3-T MR scanner (Ingenia, Philips Medical Systems, Best, The Netherlands) with a dedicated 16-channel bilateral breast coil with the patient in the prone position. Sequences included a three-plane localizing sequence, axial bilateral modified Dixon turbo spin echo T2-weighted sequences and axial T1-weighted fat-suppressed dynamic contrast-enhanced sequence with one pre-contrast and six post-contrast acquisitions. A diffusion MRI study was performed before dynamic contrast enhanced MRI, using a single-shot spin-echo EPI pulse sequence with the scan parameters shown in Table 1. Sensitizing diffusion gradients were applied in three orthogonal directions and trace-weighted diffusion-weighted images were generated.

Table 1
Diffusion weighted imaging (DWI) sequence used for conventional DWI and diffusion kurtosis imaging.

Parameter	Diffusion sequence
Sequence	Single-shot spin echo EPI
Orientation	Axial bilateral
TR/TE (ms)	14275/121
Fat suppression	SPAIR
Field of view (mm^2)	320 × 320
Matrix	224 × 227
Slice thickness (mm)	3
Number of signals averaged	1
Number of slices	50
Bandwidth (Hz/pixel)	1152
Scan time (min)	7:07
b-values (sec/mm^2)	0, 50, 600, 1000, 3000
Acceleration factor	2
Parallel imaging technique	Sensitivity Encoding (SENSE)

2.3. Image analysis

For a conventional DWI measure, ADC maps were generated with a set of diffusion weighting factors (*b* values) of 50, 600, and 1000 s/mm^2. For DKI, diffusivity (*D*) and kurtosis (*K*) maps were calculated with *b* values of 50, 600, 1000, 3000 s/mm^2. To obtain the DKI parameters, a voxel-by-voxel fit was performed with the signal decay modeled by the cumulant expansion of the signal [24]:

$$\mathrm{In}[S(b)] = \mathrm{In}[S(0)] - bD + \frac{1}{6}b^2D^2K + \cdots$$

where $S(b)$ is DWI signal at a particular *b* value, $S(0)$ the baseline signal without diffusion weighting, *D* diffusivity, and *K* diffusional kurtosis. *D* represents the diffusion coefficient with correction of non-Gaussian bias. *K*, the first higher-order term in the cumulant expansion, is a dimensionless parameter that quantifies deviation of water motion from a Gaussian distribution. When *K* is equal to zero, mean *D* becomes equal to ADC and indicates a perfect Gaussian distribution. A larger *K* value indicates a larger deviation of diffusion from a Gaussian pattern. ADC, *D* and *K* were estimated using the weighted linear least square method using an in-house developed software program in MATLAB (The MathWorks, Natick, MA) [25]. Prior to estimating D and K, ADC was estimated first for all voxels. Any voxel with ADC > 3.5 (higher than free water diffusivity) was not included in further analysis for D and K estimation, since such high ADC values are not physically possible and must be due to noise or any other artifact.

DWI data were analyzed by two radiologists (M.J.K and V.Y. P, with 16 years and 4 years of experience in breast imaging, respectively) to identify all lesions in consensus by reviewing the DWI images, with reference to the contrast-enhanced T1-weighted images. Regions of interest (ROI) for each lesion were manually drawn on a representative slice on DWI raw images and were copied onto diffusivity (*D*) maps and kurtosis (*K*) maps. The mean ROI size for additional suspicious lesions on preoperative breast MRI was 77.8 mm^2 (range, 18.1–447 mm^2). We also drew an ROI for each index breast cancer lesion, except for three cases in which the primary lesion had underwent surgical excision (n = 1) or vacuum-assisted biopsy (n = 2). The mean ROI size of index breast cancer lesions was 166.5 mm^2 (range, 20.3–796.5 mm^2).

2.4. Statistical analysis

Histogram analysis was applied to ADC, *D*, and *K*. The histogram measures included in this study were mean, standard deviation (SD), minimum, maximum, percentiles (10th, 25th, 50th, 75th, and 90th), kurtosis, skewness and entropy. We compared the histogram measures of ADC, *D* and *K* between benign vs. ductal carcinoma in situ (DCIS) vs. invasive breast lesions among additional suspicious lesions by using a nonparametric multiple comparison test (Kruskal-Wallis test followed by the Dunn multiple comparison test). For the parameters that showed a significant difference, we performed a receiver operating characteristic (ROC) curve analysis. Sensitivity and specificity were calculated with a threshold criterion determined by using the maximum Youden index. Correlation between the mean values of *D* and *K* was analyzed by Spearman coefficient (*rs*) according to lesion type. In addition, for 40 additional suspicious lesions which were detected in patients with invasive index breast cancer, correlations of the mean values of ADC, D and K between the index cancer and additional suspicious lesions were analyzed using the Spearman coefficient (*rs*) according to lesion type.

A two-tailed *P*-value of < 0.05 was considered to indicate a statistically significant difference. Statistical analyses were conducted using SPSS for Windows, version 23.0 (IBM corporation, Armonk, NY) and MedCalc Statistical Software version 18.2.1 (MedCalc Software bvba,

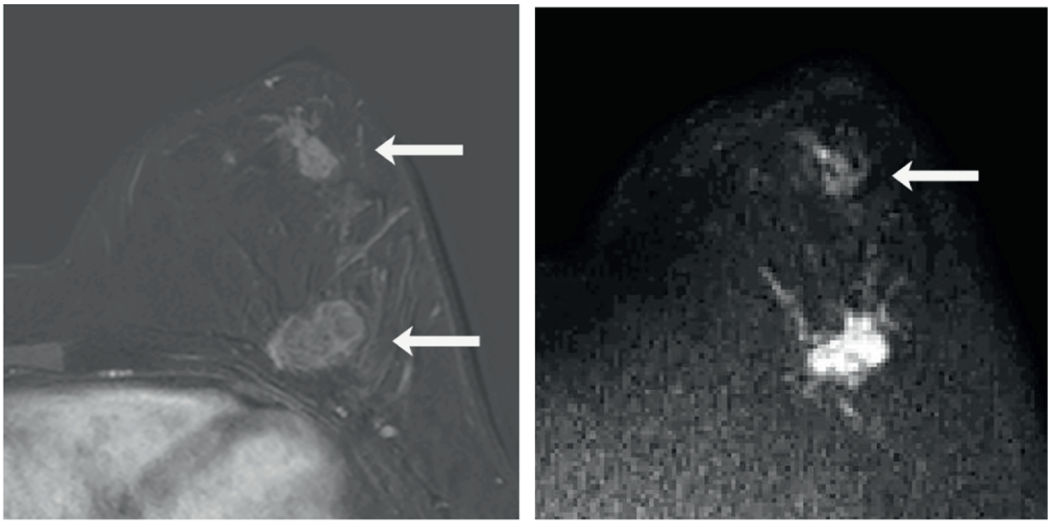

a b

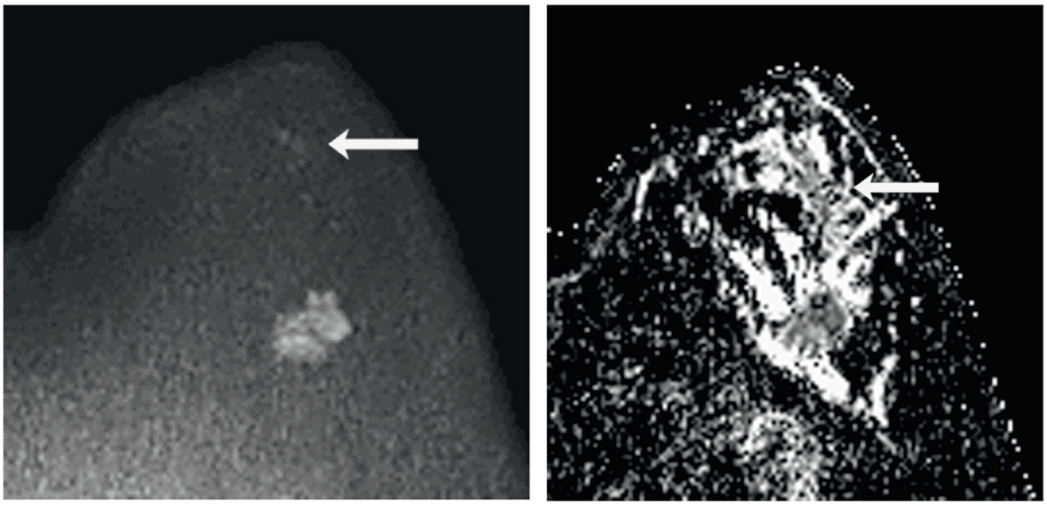

c d

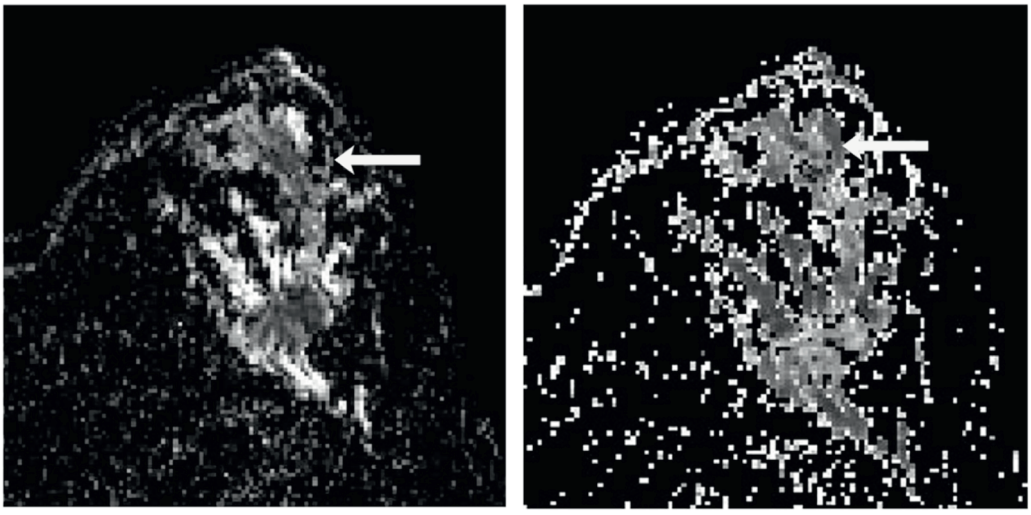

e f

(caption on next page)

Fig. 1. Images in a 45-year-old woman with an additional MR-detected suspicious lesion in the left subareolar breast. (a) Axial T1-weighted contrast-enhanced subtracted MR images show the main 32-mm invasive breast cancer at the left outer central breast (posterior arrow) and a 15-mm suspicious lesion (anterior arrow) in the left subareolar breast, which was additionally detected on preoperative breast MR imaging. DWI image with b-values of 1000 s/mm^2 (b) and 3000 s/mm^2 (c) show the left subareolar breast lesion (arrow) as hyperintense. ADC (d) and diffusivity (e) maps, respectively, show decreased signal intensity of the left subareolar breast lesion (arrow) compared with surrounding glandular tissue. (f) Kurtosis map shows that the lesion is slightly hyperintense. The lesion was surgically confirmed as ductal carcinoma in situ.

Ostend, Belgium).

3. Results

3.1. Lesion characteristics

Of the 53 pathologically confirmed additional suspicious lesions detected on preoperative breast MR imaging, 23 (43.4%) were benign and 30 (56.6%) lesions were malignant. The benign lesions consisted of fibroadenomas (n = 7), fibroadenomatous hyperplasia (n = 7), fibrocystic disease (n = 3), sclerosing adenosis (n = 1), intraductal papillomas (n = 2), radial scar (n = 1), atypical ductal hyperplasia (n = 1) and lobular carcinoma in situ (n = 1). The malignant lesions included ductal carcinoma in situ (n = 14, 46.7%) and invasive breast cancer (n = 16, 53.3%) [invasive ductal carcinoma (n = 11), invasive lobular carcinoma (n = 3) and mucinous carcinoma (n = 2)] (Figs. 1, 2). All of the malignant lesions and 5 (21.7%, including lobular carcinoma in situ [n = 1] and atypical ductal hyperplasia [n = 1]) of the benign lesions underwent surgical excision. The median follow-up period for benign breast lesions was 25.0 months (range, 5.8–40.1 months). The median lesion size on MRI was 12 mm (range, 10–92 mm).

Of the 45 index breast cancer lesions, 35 lesions were invasive breast cancer (invasive ductal carcinoma [n = 30], invasive lobular carcinoma [n = 2], mucinous carcinoma [n = 2], invasive micropapillary carcinoma [n = 1]) and 10 lesions were ductal carcinoma in situ. Among the 10 index DCIS lesions, three had underwent surgical excision (n = 1) or vacuum-assisted biopsy (n = 2), and were therefore excluded from ROI and statistical analysis.

3.2. Comparison of ADC and DKI: Benign vs. DCIS vs. invasive breast cancer

When comparing ADC histogram parameters among benign vs. DCIS vs. invasive breast cancer, the Kruskal-Wallis test showed significant differences in the mean (P = 0.028), 50th percentile (P = 0.048), 75th percentile (P = 0.014) and 90th percentile (P = 0.037) of ADC between them (Table 2). Results of multiple comparison testing showed that the mean ADC in invasive cancer tended to be lower than that of benign breast lesions (P = 0.059) and DCIS (P = 0.059). The 50th percentile of ADC in invasive breast cancer tended to be lower than that of benign lesions (P = 0.059). The 75th percentile of ADC in invasive breast cancer was significantly lower than that of both benign breast lesions (P = 0.027) and DCIS (P = 0.041). The 90th percentile of ADC in invasive breast cancer was significantly lower than that of DCIS (P = 0.038), but did not significantly differ with that of benign lesions. None of the ADC histogram parameters showed a significant difference between benign lesions and DCIS.

When comparing D histogram parameters between the three groups, the Kruskal-Wallis test showed significant differences in the mean (P = 0.014), 25th percentile (P = 0.038), 50th percentile (P = 0.011), 75th percentile (P = 0.016), 90th percentile (P = 0.024), and entropy (P = 0.015) of D between them (Table 3). Results of multiple comparison testing showed that the mean (P = 0.017), 25th percentile (P = 0.034), 50th percentile (P = 0.013), 75th percentile, and entropy (P = 0.013) of D in invasive breast cancer were lower than benign lesions. The 90th percentile of D in invasive breast cancer tended to be lower than benign lesions (P = 0.066), but showed a significant difference with that of DCIS (P = 0.040). The 50th percentile (P = 0.059) and 75th percentile (P = 0.053) of D in invasive breast cancer tended to be lower than that of DCIS.

When comparing K histogram parameters between the three groups, the Kruskal-Wallis test showed a significant difference in the 10th percentile of K (P = 0.048). When performing multiple comparisons testing, the 10th percentile of K tended to be higher in benign lesions (P = 0.059), but none showed a significant difference.

The AUC for discriminating between benign lesions and invasive cancer ranged from 0.723 to 0.758 (x10^{-3} mm^2/s) for the mean, 50th percentile, 75th percentile, and entropy of D, with high values of specificity ranging from 91.3% to 95.7% (Table 4). The AUC for the 75th percentile of ADC was 0.750, with a specificity of 100%. For distinguishing invasive cancer from DCIS lesions, the AUC values were 0.768, 0.748 and 0.732 for the 75th of ADC, 90th percentile of ADC and the 90th percentile of D respectively, with lower values of specificity ranging from 71.43% to 85.71%.

3.3. Correlation between D and K according to pathology

The mean values of D and K showed strong correlation in all lesions (r_s = −0.684, P < 0.001), and very strong correlation in benign (r_s = −0.813, P < 0.001) and invasive breast lesions (r_s = −0.853, P < 0.001) (Fig. 3). There was no significant correlation between mean values of D and K among DCIS lesions (P = 0.589). There was one outlier among the invasive additional breast lesions, which showed a high mean D value of 2.91 (x10^{-3} mm^2/s) and a low K value of 0.382. This lesion was confirmed as mucinous carcinoma, which was the same pathology as the index cancer lesion.

3.4. Correlation of ADC, D, and K between additional suspicious breast lesions and invasive index breast cancers

Among the 40 additional suspicious lesions that were detected in patients with invasive index breast cancer, the mean values of ADC, D and K showed very strong to strong correlation between invasive additional and index breast cancer lesions (ADC, r_s = 0.815, P < 0.001; D, r_s = 0.823, P < 0.001; K, r_s = 0.744, P = 0.001) (Fig. 4). However, there was no correlation between mean values of ADC, D and K between additional suspicious lesions that were confirmed as benign and index invasive breast cancer lesions (ADC, r_s = 0.256, P = 0.399; D, r_s = 0.275, P = 0.363; K, r_s = 0.143, P = 0.641), or between additional DCIS lesions and index invasive breast cancer lesions (ADC, r_s = 0.077, P = 0.821; D, r_s = 0.292, P = 0.384; K, r_s = −0.009, P = 0.979).

4. Discussion

Although unexpected additional suspicious breast lesions are detected in approximately 8%–25% of patients undergoing preoperative MR imaging [26–28], the reported specificity of DCE-MR imaging is relatively variable. To improve its diagnostic performance, several researchers have investigated whether quantitative ADC parameters can aid in predicting additional malignancy in patients with known breast cancer [28,29]. Additional malignant lesions were reported to have lower mean ADC values than benign lesions, with AUC values of mean ADC ranging from 0.76 to 0.81. However, the majority of additional malignant lesions in previous studies were invasive breast cancer, with DCIS accounting for only about 13% [28,29]. In our study, 46.7% of the

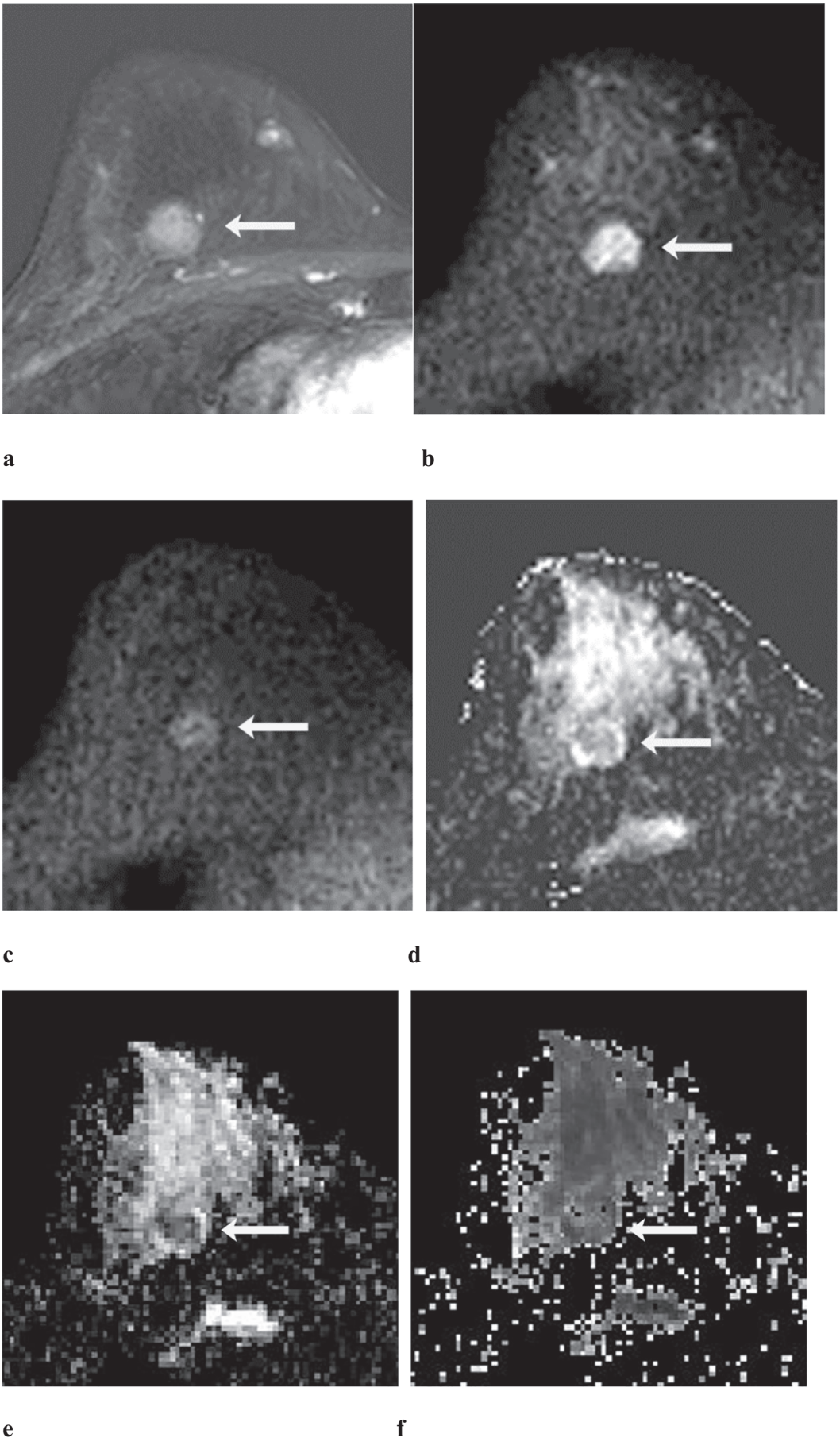

(caption on next page)

Fig. 2. Images in a 40-year-old woman with newly diagnosed breast cancer who underwent preoperative MR imaging. (a) Axial T1-weighted contrast-enhanced subtracted MR image shows an additionally detected lesion in the right lower central breast (arrow). DWI images with b-values of 1000 s/mm^2 (b) and 3000 s/mm^2 (c) show the right lower central breast lesion (arrow) is hyperintense. ADC (d), diffusivity (e) and kurtosis maps (f), respectively, show the right lower central breast lesion. The lesion was surgically confirmed as an intraductal papilloma with infarcted feature.

Table 2
Comparison of ADC histogram parameters between benign vs. DCIS vs. invasive breast cancer.

	Benign (n = 23)	DCIS (n = 14)	Invasive (n = 16)	*P* value	P value[a]		
					Benign vs. DCIS	Benign vs. Invasive	DCIS vs. Invasive
Size (mm)	12.0 (10–50)	13.5 (10–92)	12.0 (10 − 30)	0.458			
ADC parameter (10^{-3} mm^2/s)							
Mean	1.04 (0.68–2.09)	1.10 (0.79–1.33)	0.83 (0.52–2.30)	0.028	> 0.999	0.059	0.059
SD	0.33 (0.11–0.47)	0.39 (0.19–0.58)	0.30 (0.06–0.53)	0.074			
Minimum	0.42 (0–1.77)	0.27 (0.01–0.81)	0.28 (0–1.61)	0.644			
Maximum	1.70 (1.10–2.65)	1.89 (1.19–2.79)	1.43 (0.87–2.94)	0.125			
10th percentile	0.67 (0.04–1.88)	0.59 (0.05–0.87)	0.48 (0.11–1.77)	0.317			
25th percentile	0.84 (0.34–1.97)	0.84 (0.48–1.01)	0.66 (0.26–2.16)	0.118			
50th percentile	1.04 (0.66–2.08)	1.06 (0.83–1.26)	0.81 (0.49–2.27)	0.048	> 0.999	0.059	0.1689
75th percentile	1.22 (0.98–2.21)	1.39 (0.92–1.63)	0.96 (0.66–2.44)	0.014	> 0.999	0.027	0.041
90th percentile	1.40 (1.02–2.32)	1.56 (1.05–2.25)	1.21 (0.84–2.61)	0.037	> 0.999	0.202	0.038
Kurtosis	2.85 (2.04–8.23)	2.70 (1.71–3.96)	3.10 (2.09–4.91)	0.599			
Skewness	− 0.13 (− 1.92–1.94)	0.28 (− 0.63–0.84)	0.11 (− 0.94–1.24)	0.084			
Entropy	2.69 (0–4.77)	2.59 (1.26–4.68)	3.45 (0–5.6)	0.089			

[a] Calculated with the Kruskal-Wallis test followed by the Dunn multiple comparisons test.

Table 3
Comparison of DKI (diffusivity and kurtosis) histogram parameters between benign vs. DCIS. vs. invasive breast cancer.

	Benign (n = 23)	DCIS (n = 14)	Invasive (n = 16)	P value	P value[a]		
					Benign vs. DCIS	Benign vs. Invasive	DCIS vs. Invasive
Diffusivity (*D*) (10^{-3} mm^2/s)							
Mean	1.35 (0.90–2.45)	1.36 (0.98–1.70)	0.98 (0.62–2.91)	0.014	> 0.999	0.017	0.074
SD	0.46 (0.11–0.63)	0.57 (0.24–0.87)	0.42 (0.10–0.66)	0.143			
Minimum	0.42 (0–2.05)	0.27 (0.01–0.97)	0.28 (0–1.64)	0.634			
Maximum	2.35 (1.24–3.40)	2.37 (1.46–3.35)	1.87 (1.05–4.60)	0.075			
10th percentile	0.80 (0.04–2.23)	0.66 (0.05–1.01)	0.53 (0.11–2.23)	0.320			
25th percentile	1.07 (0.34–2.31)	1.05 (0.48–1.26)	0.79 (0.26–2.58)	0.038	> 0.999	0.034	0.316
50th percentile	1.35 (0.82–2.45)	1.36 (1.01–1.55)	0.99 (0.44–2.80)	0.011	0.832	0.013	0.059
75th percentile	1.56 (1.15–2.58)	1.71 (1.21–2.34)	1.20 (0.84–3.06)	0.016	> 0.999	0.027	0.053
90th percentile	1.90 (1.22–2.82)	2.00 (1.30–2.83)	1.56 (1.00–3.73)	0.024	> 0.999	0.066	0.040
Kurtosis	3.03 (1.86–7.96)	3.05 (1.64–5.19)	2.92 (2.12–6.13)	0.763	0.769		
Skewness	− 0.14 (− 1.56–1.78)	0.07 (− 0.58–1.13)	0.34 (− 0.80–2.26)	0.196	0.526		
Entropy	1.37 (0–3.69)	1.46 (0.64–2.99)	3.17 (0–5.07)	0.015	> 0.999	0.013	> 0.999
DKI Kurtosis (*K*)							
Mean	0.84 (0.40–1.17)	0.81 (0.61–1.00)	0.83 (0.38–1.39)	0.696			
SD	0.17 (0.02–0.47)	0.23 (0.12–0.31)	0.20 (0.05–0.38)	0.133			
Minimum	0.52 (0.22–0.80)	0.43 (0.04–0.72)	0.54 (0.05–0.81)	0.253			
Maximum	1.16 (0.43–2.52)	1.26 (0.90–1.94)	1.24 (0.53–2.26)	0.834			
10th percentile	0.63 (0.34–0.84)	0.50 (0.19–0.75)	0.64 (0.05–0.88)	0.048	0.059	> 0.999	0.136
25th percentile	0.71 (0.36–0.97)	0.63 (0.43–0.88)	0.71 (0.35–1.06)	0.188			
50th percentile	0.80 (0.40–1.16)	0.77 (0.61–0.98)	0.83 (0.38–1.39)	0.540			
75th percentile	0.94 (0.41–1.30)	0.94 (0.77–1.13)	0.93 (0.40–1.57)	0.745			
90th percentile	1.06 (0.42–1.57)	1.03 (0.81–1.45)	1.00 (0.41–1.77)	0.829			
Kurtosis	3.44 (1.49–17.87)	3.66 (1.67–11.72)	3.14 (1.57–10.02)	0.962			
Skewness	0.34 (− 1.88–3.64)	0.40 (− 2.70–1.45)	0.17 (− 2.49–1.66)	0.560			
Entropy	3.81 (1.56–5.82)	4.21 (2.35–5.56)	3.74 (0.64–5.59)	0.521			

[a] Calculated with the Kruskal-Wallis test followed by the Dunn multiple comparisons test.

malignant breast lesions were DCIS and there was no significant difference in mean ADC values between DCIS and benign breast lesions. Therefore, our results may imply that mean values of ADC would be less helpful for evaluating additionally detected lesions on preoperative MRI in patient groups that have a high prevalence of DCIS or when accurate identification of DCIS is critical.

Recently, ADC histogram analysis has also been applied for the characterization of index breast lesions [30–32]. Previous researchers have reported a higher diagnostic performance of minimum ADC than mean ADC in slightly larger studies comprised of 75 to 101 patients, in which DCIS accounted for 4%–14% of index malignant breast lesions [31,32]. In our study, although the minimum ADC did not significantly differ according to pathology, several other ADC histogram parameters showed a significant difference between benign vs. invasive and DCIS vs. invasive cancer, also suggesting that ADC histogram analysis could aid in characterization of additional suspicious lesions at preoperative breast MR imaging.

DKI has recently been investigated as another adjunctive method to improve the performance of breast DCE-MR imaging, mainly by increasing its specificity [19,20]. The reported AUCs of *D* for the

Table 4
ROC curve analysis of ADC, DKI histogram measures which showed a significant difference according to pathology.

Benign vs. Invasive	ADC-75th percentile	*D*-Mean	*D*-25th percentile	*D*-50th percentile	*D*-75thpercentile	*D*-Entropy
Threshold (10^{-3} mm^2/s)	≤0.965	≤1.065	≤0.939	≤1.002	≤1.234	> 2.581
AUC	0.750	0.755	0.723	0.753	0.750	0.758
Sensitivity (%)	56.2%	62.5%	75.0%	62.5%	56.2%	62.5%
Specificity (%)	100%	91.3%	69.57%	95.7%	95.7%	91.3%
P value	0.005	0.003	0.011	0.004	0.005	0.003

DCIS vs. Invasive	ADC-75th percentile	ADC-90th percentile	*D*-90th percentile
Threshold (10^{-3} mm^2/s)	≤1.297	≤1.331	≤1.764
AUC	0.768	0.748	0.732
Sensitivity (%)	81.25%	68.75%	75.0%
Specificity (%)	71.43%	85.71%	78.6%
P value	0.004	0.009	0.019

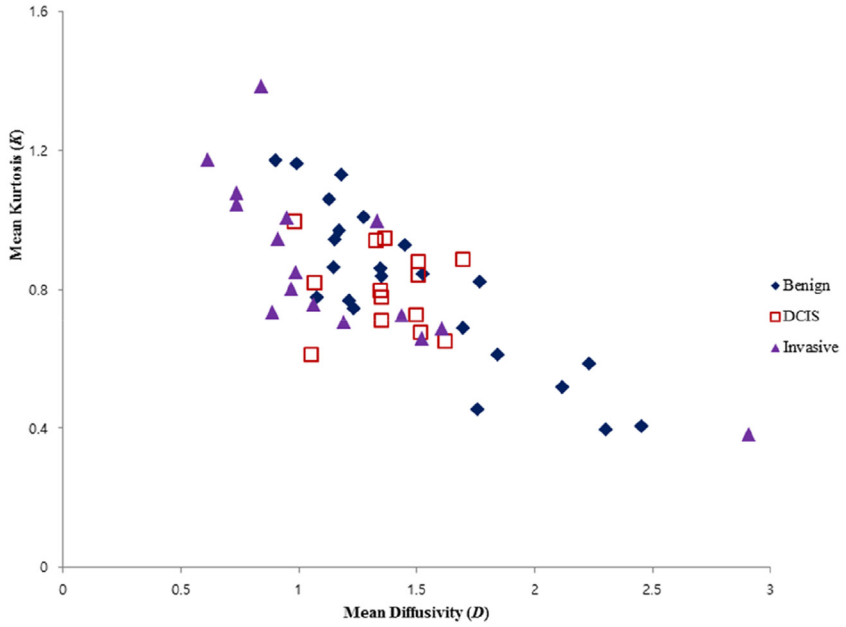

Fig. 3. Scatter plot shows negative correlation between the mean values of *D* (10^{-3} mm^2/s) and *K* in benign and invasive breast lesions, but no correlation in DCIS lesions.

differentiation of benign and malignant breast lesions range between approximately 0.95 to 0.97, respectively [19,20,33,34]. As previous studies had included main breast lesions that were considered suspicious at mammography or US, the average lesion size was larger than that in our study − especially for malignant lesions, which ranged from 24 to 36 mm [19,20,33]. In addition, the majority of malignant lesions in previous studies were invasive breast cancer. Such differences in lesion type and size would be expected, as additionally detected suspicious lesions at preoperative imaging would more likely be smaller and have a higher proportion of DCIS than index cancers [12]. The lower performance of DKI in our study compared to previous reports would be at least partially attributed to differences in the study population [17–20,35]. Furthermore, *K* histogram parameters failed to show a significant difference at multiple comparisons. Although the application of diffusion gradients in three orthogonal directions to generate trace-weighted images is the standard imaging protocol in body DWI and has been used in previous breast DKI studies [18,19,34], recent research has reported that the use of trace-weighted images can introduce both bias and error in the estimation of DKI-derived indices, especially for *K* values [36,37]. As it has been shown that water diffusion in breast tissue is not isotropic [38,39], the use of only three diffusion weighting directions would not allow a rotational invariant estimation of diffusion kurtosis. For a rigorous estimation, a protocol including at least 15 diffusion weighting directions and 2 non-null b-values would be required [40]. Furthermore, although we applied a high b value of 3000 based on earlier studies utilizing DKI analysis [18,19,41], this does not necessarily suggest that the b values used were optimal for accurate DKI analysis. These factors may have further affected the performance of DKI analysis in our study. In addition, non-linearity of diffusion gradients and eddy current-induced distortions have been shown to cause inaccuracy in quantitative DWI [42–46], and further improvement in future studies may be achieved by applying gradient non-linearity and eddy current distortion correction.

When performing multiple comparisons between additional benign vs. DCIS vs. invasive breast lesions, we found that the mean ADC values tended to be lower in invasive breast cancer than benign lesions or DCIS lesions. We found that the mean *D* value in invasive breast cancer was significantly lower than that of benign lesions ($P = 0.017$) and tended to be lower than that of DCIS ($P = 0.074$). However, neither differed between benign and DCIS lesions. Histogram analysis showed that multiple *D* histogram parameters (25th, 50th, 75th and 90th percentile and entropy) and two ADC histogram parameters differed between invasive cancer vs. benign or invasive cancer vs. DCIS. However, none of the histogram parameters showed a significant difference between benign and DCIS lesions. As *D* histogram parameters that significantly differed according to pathology showed similar diagnostic performance

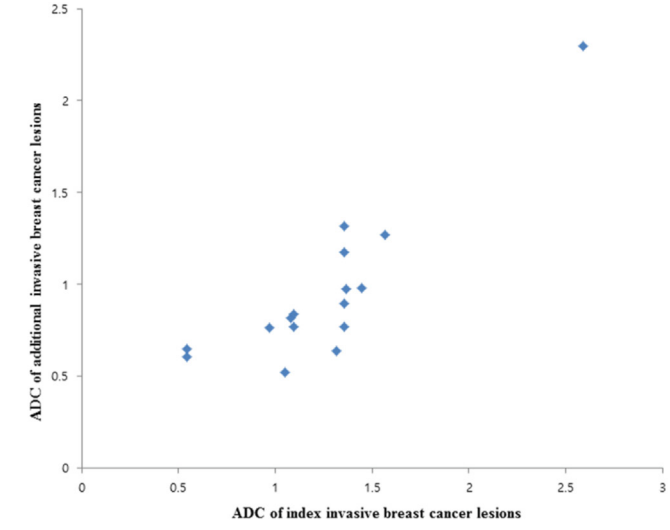

a

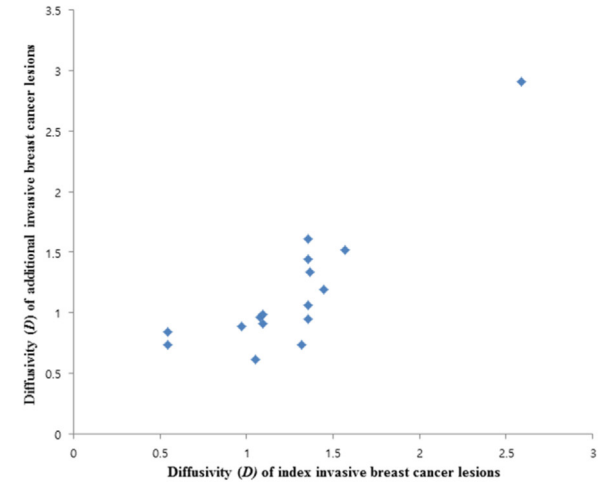

b

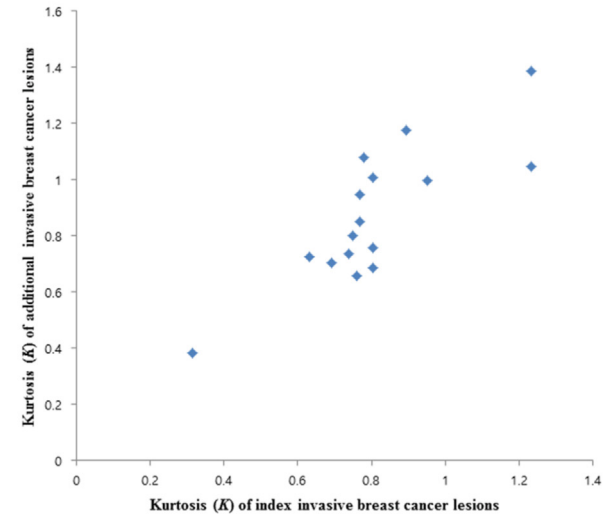

c

Fig. 4. Scatter plot shows correlation of mean values of ADC (10^{-3} mm^2/s) (a), diffusivity (D) (10^{-3} mm^2/s) (b), and kurtosis (K) (c) between the invasive index and invasive additional breast cancer lesions in 16 patients.

with significant ADC histogram parameters, it may be implied that although DKI analysis can help differentiate between benign and malignant additional lesions detected on preoperative breast MRI imaging, it may have little additional value to conventional ADC analysis.

Similarly, when performing correlation analysis between additional suspicious breast lesions and index invasive breast cancer, we found that although the mean values of ADC, D, and K showed very strong correlation between invasive additional and index breast cancer lesions, there was no correlation between mean values of ADC, D, and K between additional benign/DCIS lesions and invasive index breast cancer. Our results suggest that the histologic type could be the primary factor affecting ADC and DKI parameters. In addition, although the mean values of D and K showed very strong correlation in additional benign and invasive breast lesions, no significant correlation was seen in DCIS. We speculate that possibly due to inherent heterogeneity of DCIS, other factors in addition to non-Gaussian distribution may affect D or K in this subgroup. Our results suggest that when evaluating additional suspicious lesions on preoperative breast MR imaging, DKI may help lesion characterization. Yet, differentiating DCIS from benign lesions would still be difficult and thus, could limit its role in this subgroup. In contrast, we anticipate that DKI could have a higher potential in future non-contrast screening breast MR imaging, by aiding in the detection of small invasive breast cancers that would be more likely clinically significant than small DCIS.

Our study had several limitations. First, this was a single-center study and the number of included patients was small. Second, the retrospective study design and inclusion of lesions larger than 10 mm would have inevitably led to selection bias. Such a size criterion would limit its range of application in clinical practice, as a large portion of additional MR-detected lesions are small and caused us to include only a quarter of initially eligible lesions. However, such a size threshold is a common approach in exploratory studies investigating the potential of diffusion-weighted imaging techniques, and would allow further expansion to smaller lesions in future studies [47,48]. Third, ROIs were manually drawn on a representative slice, and whole-volume lesion analysis was not performed. Although previous studies on DKI have also used this approach, this could have affected results of histogram analysis [18,33]. Fourth, DKI and ADC analysis were based on datasets with different acquisition times. Although this would have allowed comparison with conventional DWI used in clinical practice, it would have caused bias in the comparison between the two diffusion-MRI techniques. Fifth, a specific quality control program for evaluation of MR scanner system-related factors in diffusion indices was not performed prior to the initiation of the study. Such quality assurance procedures have been recently emphasized in order to guarantee accurate and reproducible diffusion measurements, and would be recommended in future diffusion-MRI studies [49–52]. Sixth, imaging processing to correct diffusion-weighted images for eddy current induced distortion was not performed. Finally, our study population had a high proportion of DCIS (46.7% among malignant lesions) compared with previous studies on DKI and DWI imaging. However, this likely represents the characteristics of additional suspicious lesions detected at preoperative breast imaging, and would be informative when considering its application in this subgroup.

5. Conclusion

In conclusion, our study shows that DKI analysis may aid in the differentiation of additional suspicious lesions detected on preoperative breast MR imaging, but may have little additional value to ADC analysis. Both ADC and DKI may have lower potential in differentiating

DCIS from benign lesions, and further studies are required to evaluate its role in this subgroup.

Acknowledgements

Funding

This study was supported by a Basic Science Research Program through the National Research Foundation of Korea (NRF) funded by the Ministry of Education (NRF-2017R1D1A1B03035995) and by the Basic Science Research Program through the National Research Foundation of Korea (NRF) funded by the Ministry of Science, ICT & Future Planning, Republic of Korea (NRF-2017R1A2B4010407).

References

[1] Berg WA, Gutierrez L, NessAiver MS, Carter WB, Bhargavan M, Lewis RS, et al. Diagnostic accuracy of mammography, clinical examination, US, and MR imaging in preoperative assessment of breast cancer. Radiology 2004;233:830–49.
[2] Sardanelli F, Podo F, Santoro F, Manoukian S, Bergonzi S, Trecate G, et al. Multicenter surveillance of women at high genetic breast cancer risk using mammography, ultrasonography, and contrast-enhanced magnetic resonance imaging (the high breast cancer risk italian 1 study): final results. Invest Radiol 2011;46:94–105.
[3] Liberman L, Morris EA, Kim CM, Kaplan JB, Abramson AF, Menell JH, et al. MR imaging findings in the contralateral breast of women with recently diagnosed breast cancer. AJR Am J Roentgenol 2003;180:333–41.
[4] Lehman CD, Gatsonis C, Kuhl CK, Hendrick RE, Pisano ED, Hanna L, et al. MRI evaluation of the contralateral breast in women with recently diagnosed breast cancer. N Engl J Med 2007;356:1295–303.
[5] Brennan ME, Houssami N, Lord S, Macaskill P, Irwig L, Dixon JM, et al. Magnetic resonance imaging screening of the contralateral breast in women with newly diagnosed breast cancer: systematic review and meta-analysis of incremental cancer detection and impact on surgical management. J Clin Oncol 2009;27:5640–9.
[6] Plana MN, Carreira C, Muriel A, Chiva M, Abraira V, Emparanza JI, et al. Magnetic resonance imaging in the preoperative assessment of patients with primary breast cancer: systematic review of diagnostic accuracy and meta-analysis. Eur Radiol 2012;22:26–38.
[7] El Sharouni MA, Postma EL, Menezes GL, van den Bosch MA, Pijnappel RM, Witkamp AJ, et al. High prevalence of MRI-detected contralateral and ipsilateral malignant findings in patients with invasive ductolobular breast cancer: impact on surgical management. Clin Breast Cancer 2016;16:269–75.
[8] Wang SY, Long JB, Killelea BK, Evans SB, Roberts KB, Silber A, et al. Preoperative breast magnetic resonance imaging and contralateral breast cancer occurrence among older women with breast cancer. J Clin Oncol 2016;34:321–8.
[9] Jonna AR, Sam KQ, Ebuoma LO, Sedgwick EL, Wang T, Benveniste AP. Detection of multicentric and contralateral breast cancers on MRI based on primary cancer biomarker status: will this change surgical or medical management? Breast Cancer Res Treat 2017;166:623–9.
[10] Lobbes MB, Vriens IJ, van Bommel AC, Nieuwenhuijzen GA, Smidt ML, Boersma LJ, et al. Breast MRI increases the number of mastectomies for ductal cancers, but decreases them for lobular cancers. Breast Cancer Res Treat 2017;162:353–64.
[11] Vapiwala N, Hwang WT, Kushner CJ, Schnall MD, Freedman GM, Solin LJ. No impact of breast magnetic resonance imaging on 15-year outcomes in patients with ductal carcinoma in situ or early-stage invasive breast cancer managed with breast conservation therapy. Cancer 2017;123:1324–32.
[12] Iacconi C, Galman L, Zheng J, Sacchini V, Sutton EJ, Dershaw D, et al. Multicentric cancer detected at breast MR imaging and not at mammography: important or not? Radiology 2016;279:378–84.
[13] Houssami N, Ciatto S, Macaskill P, Lord SJ, Warren RM, Dixon JM, et al. Accuracy and surgical impact of magnetic resonance imaging in breast cancer staging: systematic review and meta-analysis in detection of multifocal and multicentric cancer. J Clin Oncol 2008;26:3248–58.
[14] Ei Khouli RH, Jacobs MA, Mezban SD, Huang P, Kamel IR, Macura KJ, et al. Diffusion-weighted imaging improves the diagnostic accuracy of conventional 3.0-T breast MR imaging. Radiology 2010;256:64–73.
[15] Bickelhaupt S, Laun FB, Tesdorff J, Lederer W, Daniel H, Stieber A, et al. Fast and noninvasive characterization of suspicious lesions detected at breast cancer X-ray screening: capability of diffusion-weighted MR imaging with MIPs. Radiology 2016;278:689–97.
[16] Bogner W, Gruber S, Pinker K, Grabner G, Stadlbauer A, Weber M, et al. Diffusion-weighted MR for differentiation of breast lesions at 3.0 T: how does selection of diffusion protocols affect diagnosis? Radiology 2009;253:341–51.
[17] Wu D, Li G, Zhang J, Chang S, Hu J, Dai Y. Characterization of breast tumors using diffusion kurtosis imaging (DKI). PLoS One 2014;9:e113240.
[18] Nogueira L, Brandao S, Matos E, Nunes RG, Loureiro J, Ramos I, et al. Application of the diffusion kurtosis model for the study of breast lesions. Eur Radiol 2014;24:1197–203.
[19] Sun K, Chen X, Chai W, Fei X, Fu C, Yan X, et al. Breast cancer: diffusion kurtosis MR imaging-diagnostic accuracy and correlation with clinical-pathologic factors. Radiology 2015;277:46–55.
[20] Christou A, Ghiatas A, Priovolos D, Veliou K, Bougias H. Accuracy of diffusion kurtosis imaging in characterization of breast lesions. Br J Radiol 2017;90:20160873.
[21] Partridge SC, McDonald ES. Diffusion weighted magnetic resonance imaging of the breast: protocol optimization, interpretation, and clinical applications. Magn Reson Imaging Clin N Am 2013;21:601–24.
[22] Thomassin-Naggara I, De Bazelaire C, Chopier J, Bazot M, Marsault C, Trop I. Diffusion-weighted MR imaging of the breast: advantages and pitfalls. Eur J Radiol 2013;82:435–43.
[23] Brandao AC, Lehman CD, Partridge SC. Breast magnetic resonance imaging: diffusion-weighted imaging. Magn Reson Imaging Clin N Am 2013;21:321–36.
[24] Jensen JH, Helpern JA, Ramani A, Lu H, Kaczynski K. Diffusional kurtosis imaging: the quantification of non-gaussian water diffusion by means of magnetic resonance imaging. Magn Reson Med 2005;53:1432–40.
[25] Veraart J, Sijbers J, Sunaert S, Leemans A, Jeurissen B. Weighted linear least squares estimation of diffusion MRI parameters: strengths, limitations, and pitfalls. Neuroimage 2013;81:335–46.
[26] Lee SH, Kim SM, Jang M, Yun BL, Kang E, Kim SW, et al. Role of second-look ultrasound examinations for MR-detected lesions in patients with breast cancer. Ultraschall Med 2015;36:140–8.
[27] Park VY, Kim MJ, Moon HJ, Kim EK. Additional malignant breast lesions detected on second-look US after breast MRI vs. additional malignant lesions detected on initial US in breast cancer patients: comparison of US characteristics. Ultraschall Med 2014;35:432–9.
[28] Yoo H, Shin HJ, Baek S, Cha JH, Kim H, Chae EY, et al. Diagnostic performance of apparent diffusion coefficient and quantitative kinetic parameters for predicting additional malignancy in patients with newly diagnosed breast cancer. Magn Reson Imaging 2014;32:867–74.
[29] Song SE, Park EK, Cho KR, Seo BK, Woo OH, Jung SP, et al. Additional value of diffusion-weighted imaging to evaluate multifocal and multicentric breast cancer detected using pre-operative breast MRI. Eur Radiol 2017;27:4819–27.
[30] Park GE, Kim SH, Kim EJ, Kang BJ, Park MS. Histogram analysis of volume-based apparent diffusion coefficient in breast cancer. Acta Radiol 2017;58:1294–302.
[31] Suo S, Zhang K, Cao M, Suo X, Hua J, Geng X, et al. Characterization of breast masses as benign or malignant at 3.0T MRI with whole-lesion histogram analysis of the apparent diffusion coefficient. J Magn Reson Imaging 2016;43:894–902.
[32] Hirano M, Satake H, Ishigaki S, Ikeda M, Kawai H, Naganawa S. Diffusion-weighted imaging of breast masses: comparison of diagnostic performance using various apparent diffusion coefficient parameters. AJR Am J Roentgenol 2012;198:717–22.
[33] Iima M, Yano K, Kataoka M, Umehana M, Murata K, Kanao S, et al. Quantitative non-Gaussian diffusion and intravoxel incoherent motion magnetic resonance imaging: differentiation of malignant and benign breast lesions. Invest Radiol 2015;50:205–11.
[34] Suo S, Cheng F, Cao M, Kang J, Wang M, Hua J, et al. Multiparametric diffusion-weighted imaging in breast lesions: association with pathologic diagnosis and prognostic factors. J Magn Reson Imaging 2017;46:740–50.
[35] Bickelhaupt S, Jaeger PF, Laun FB, Lederer W, Daniel H, Kuder TA, et al. Radiomics Based on Adapted Diffusion Kurtosis Imaging Helps to Clarify Most Mammographic Findings Suspicious for Cancer. Radiology 2018;287:761–70.
[36] Marzi S, Minosse S, Vidiri A, Piludu F, Giannelli M. Diffusional kurtosis imaging in head and neck cancer: on the use of trace-weighted images to estimate indices of non-Gaussian water diffusion. Med Phys 2018;45:5411–9.
[37] Giannelli M, Toschi N. On the use of trace-weighted images in body diffusional kurtosis imaging. Magn Reson Imaging 2016;34:502–7.
[38] Eyal E, Shapiro-Feinberg M, Furman-Haran E, Grobgeld D, Golan T, Itzchak Y, et al. Parametric diffusion tensor imaging of the breast. Invest Radiol 2012;47:284–91.
[39] Furman-Haran E, Grobgeld D, Nissan N, Shapiro-Feinberg M, Degani H. Can diffusion tensor anisotropy indices assist in breast cancer detection? J Magn Reson Imaging 2016;44:1624–32.
[40] Jensen JH, Helpern JA. MRI quantification of non-Gaussian water diffusion by kurtosis analysis. NMR Biomed 2010;23:698–710.
[41] Li T, Yu T, Li L, Lu L, Zhuo Y, Lian J, et al. Use of diffusion kurtosis imaging and quantitative dynamic contrast-enhanced MRI for the differentiation of breast tumors. J Magn Reson Imaging 2018;48:1358–66.
[42] Tan ET, Marinelli L, Slavens ZW, King KF, Hardy CJ. Improved correction for gradient nonlinearity effects in diffusion-weighted imaging. J Magn Reson Imaging 2013;38:448–53.
[43] Newitt DC, Tan ET, Wilmes LJ, Chenevert TL, Kornak J, Marinelli L, et al. Gradient nonlinearity correction to improve apparent diffusion coefficient accuracy and standardization in the american college of radiology imaging network 6698 breast cancer trial. J Magn Reson Imaging 2015;42:908–19.
[44] Le Bihan D, Poupon C, Amadon A, Lethimonnier F. Artifacts and pitfalls in diffusion MRI. J Magn Reson Imaging 2006;24:478–88.
[45] Jones DK, Cercignani M. Twenty-five pitfalls in the analysis of diffusion MRI data. NMR Biomed 2010;23:803–20.
[46] Arlinghaus LR, Welch EB, Chakravarthy AB, Xu L, Farley JS, Abramson VG, et al. Motion correction in diffusion-weighted MRI of the breast at 3T. J Magn Reson Imaging 2011;33:1063–70.
[47] Rubesova E, Grell AS, De Maertelaer V, Metens T, Chao SL, Lemort M. Quantitative diffusion imaging in breast cancer: a clinical prospective study. J Magn Reson Imaging 2006;24:319–24.
[48] Marini C, Iacconi C, Giannelli M, Cilotti A, Moretti M, Bartolozzi C. Quantitative diffusion-weighted MR imaging in the differential diagnosis of breast lesion. Eur Radiol 2007;17:2646–55.
[49] Giannelli M, Sghedoni R, Iacconi C, Iori M, Traino AC, Guerrisi M, et al. MR scanner systems should be adequately characterized in diffusion-MRI of the breast. PLoS

One 2014;9:e86280.
[50] Malyarenko D, Galban CJ, Londy FJ, Meyer CR, Johnson TD, Rehemtulla A, et al. Multi-system repeatability and reproducibility of apparent diffusion coefficient measurement using an ice-water phantom. J Magn Reson Imaging 2013;37:1238–46.
[51] Belli G, Busoni S, Ciccarone A, Coniglio A, Esposito M, Giannelli M, et al. Quality assurance multicenter comparison of different MR scanners for quantitative diffusion-weighted imaging. J Magn Reson Imaging 2016;43:213–9.
[52] Shukla-Dave A, Obuchowski NA, Chenevert TL, Jambawalikar S, Schwartz LH, Malyarenko D, et al. Quantitative imaging biomarkers alliance (QIBA) recommendations for improved precision of DWI and DCE-MRI derived biomarkers in multicenter oncology trials. J Magn Reson Imaging 2019. e101-e21.